Reliability Engineering and System Safety 222 (2022) 108390

Contents lists available at ScienceDirect

Reliability Engineering and System Safety

journal homepage: www.elsevier.com/locate/ress

Optimal life-cycle mitigation of fatigue failure risk for structural systems

Jorge Mendoza [a,*], Elizabeth Bismut [b], Daniel Straub [b], Jochen Köhler [a]

[a] Norwegian University of Science and Technology, Department of Structural Engineering, 7491 Trondheim, Norway
[b] Technical University of Munich, Engineering Risk Analysis Group, 80333 Munich, Germany

ARTICLE INFO

Keywords:
Fatigue design
Inspection and maintenance
Structural reliability
Structural systems

ABSTRACT

Fatigue failure risk can be mitigated both by increasing the design fatigue capacity of the structural components and by conducting more frequent inspection and maintenance actions. The optimal combination of these two types of safety measure is structure dependent. It depends, among others, on the relative cost of the safety measures, the consequences of failure, the level of redundancy, the number of deteriorating components and the statistical dependence among components. In this article, a generic system representation is used to parametrise deteriorating structures according to these system characteristics. Based on this system representation, we investigate patterns of optimal life-cycle fatigue mitigation and provide recommendations for fatigue design. Results show that it can be cost-efficient to achieve system-level safety requirements with high component reliabilities at design and less frequent inspections. Furthermore, we show that the minimum requirements for fatigue design that are typically prescribed in design standards to avoid the need for inspections are not enough unless sufficient redundancy is ensured.

1. Introduction

The reliability of fatigue deteriorating structures can be affected by mitigation measures at different stages of their life cycle. For instance, the deteriorating components can be designed with higher or lower reliability at the design stage. Moreover, inspection and maintenance (I&M) actions can be conducted during the service life of the structure; e.g., inspections can be used to identify fatigue damage, which can then be repaired. In general, a combination of mitigation measures can be specified in order to satisfy a certain safety level during the service life of a structure. This implies that minimum requirements for fatigue design should depend on life-cycle considerations, such as how often inspections will be conducted.

Standards [1–3] and recommended practice guidelines [4,5] for the fatigue design of steel components typically prescribe different safety levels depending on the accessibility for inspections and repair. For accessible fatigue hot spots, i.e., hot spots that can be inspected, the damage-tolerant approach can be followed. According to this approach, cracks are tolerated and expected to develop and grow as long as they are controlled by a preventive I&M program. Safety requirements for component fatigue design are typically specified by the fatigue design factor, denoted FDF, which is defined as the ratio between the deterministic fatigue life T_{FL} of the component and its design service life T_{SL}, i.e., $FDF = T_{FL}/T_{SL}$. Generally, a fatigue design can be specified for a component to satisfy a FDF. For example, the diameter and wall thickness of a tubular beam can be enlarged to increase its FDF. Regarding the optimisation of the geometrical design of a component to achieve a certain FDF, the reader is referred to Schafhirt et al. [6], among others.

Although fatigue design depends on the accessibility for inspections and repair, standards and guidelines do not provide clear recommendations on how to efficiently combine design and I&M measures to mitigate fatigue failures [7,8]. The interplay between I&M and fatigue design has been addressed in the literature, mainly in relation to the offshore oil and gas industry in the 90s [9,10] and more recently, in relation to the offshore wind energy sector [11,12]. Sørensen [11] and Márquez-Domínguez and Sørensen [13] show that a significant reduction of the FDF can be tolerated by reducing the interval between inspections in an application for fatigue design of offshore wind turbines. It was found that for a target reliability index of 3.1, the FDF can be reduced from 6.1 (case with no inspections) to 1 by setting the interval between inspections to 2.5 years. An overview of relevant research on reliability and risk-based life-cycle fatigue optimisation can be found in Mendoza et al. [8], where it is concluded, in agreement with Yang et al. [14], that research in this field has typically neglected system effects. Furthermore, [8] shows that system effects should be considered to inform optimal life-cycle mitigation decisions as they affect the risk of failure and the efficiency of inspections. Similar conclusions were drawn by Moan [7], who indicated that inspection scheduling and design for robustness need to be simultaneously regarded to arrive at acceptable risks. Recent efforts have been devoted to

* Corresponding author.
E-mail address: jorge.m.espinosa@ntnu.no (J. Mendoza).

https://doi.org/10.1016/j.ress.2022.108390
Received 26 August 2021; Received in revised form 9 February 2022; Accepted 12 February 2022
Available online 26 February 2022

the modelling and reliability assessment of deteriorating systems with statistically dependent components, see among others [15–19].

The consideration of system effects and the simultaneous optimisation of design and I&M is conceptually complex and computationally demanding [8]. Therefore, the implementation of these aspects in the general engineering practice is challenging. In this paper, we simultaneously optimise the fatigue design and I&M plans for systems with varying redundancy and number of deteriorating components. These results are used to identify patterns on how these system characteristics affect the optimal fatigue mitigation strategy based on reliability and risk criteria. Based on the identified patterns, general recommendations for fatigue design are given. The methodology is presented in Section 2. So-called equivalent Daniels systems are used to parametrise structural systems according to the corresponding system features of interest and to evaluate their time-variant reliability. A parametric investigation, which is specified in Section 3, is conducted to study the optimal fatigue mitigation strategy as a function of the system parameters. The results are shown in Section 4. Practical implications of the obtained results are discussed in Section 5. The main outcomes of the article are summarised in Section 6.

2. Methodology

The aim is to investigate how the optimal life-cycle strategy to mitigate fatigue failures varies for different structural systems. Structural systems are parametrised according to relevant system features such as the level of redundancy and the number of deteriorating components. An efficient parametric representation of structural systems is presented in Section 2.1. This system representation is then used to conduct a parametric study, as described in Section 3. The considered life-cycle strategies encompass design and I&M mitigation actions, which are respectively specified by the FDF of the fatigue hot spots and the frequency between inspection campaigns. The optimality of the strategies is determined according to risk and reliability criteria. The mathematical formulation of the corresponding objective functions is presented in Section 2.2.

2.1. System idealisation with equivalent Daniels systems

Optimal fatigue mitigation depends on various system characteristics. To arrive at meaningful recommendations on how to efficiently mitigate fatigue deterioration, we study the patterns of the optimal fatigue mitigation strategy as a function of relevant system characteristics by means of a parametric study. For that purpose, structural systems are to be conveniently parametrised. The desired system parametrisation should allow to efficiently evaluate the system reliability as a function of a mitigation strategy and the system parameters.

Generically, a structural system with n components or fatigue hot spots, and subject to extreme static and cyclic loads is considered. As discussed in [20], an exact representation of the structural system, e.g., as a combination of parallel subsystems in series [21], is not conducive to general conclusions. As an alternative, the role of a given component in the structural integrity of the system can be captured by a set of features such as the importance of the component for structural integrity, the number of deteriorating components and the dependence among the deterioration processes at different locations within the structure [20].

Gharaibeh et al. [22] propose to measure the importance of a component based on the sensitivity of the system reliability to changes in the component's reliability, both in the intact and post-failure states. These measures are useful to assess design for ultimate limit state (ULS). However, they are not meaningful to assess mitigation of deterioration mechanisms because they do not measure how the system reliability is reduced by given component damage. For that purpose, we use the single element importance SEI proposed in [20]:

$$SEI_i = \Pr(F_{sys}|\bar{F}_1 \cap \ldots \cap \bar{F}_{i-1} \cap F_i \cap \bar{F}_{i+1} \cap \ldots \cap \bar{F}_n) - \Pr(F_{sys}|\cap_{j=1}^{n} \bar{F}_j), \quad (1)$$

which measures the increase of the structure's probability of failure resulting from failure of component i only. Note that F_{sys} is the event of system failure, and F_j and $\bar{F}_j$ indicate failure and survival of a component j, respectively. The undamaged probability of system failure can be alternatively expressed through the annual reliability index of the undamaged system $\beta_{\bar{D}S}$ as

$$\Pr(F_{sys}|\cap_{j=1}^{n} \bar{F}_j) = \Phi(-\beta_{\bar{D}S}), \quad (2)$$

where $\Phi(\cdot)$ is the cumulative distribution function of the standard normal distribution.

The SEI of the components, together with a joint probabilistic representation of deterioration, load, and resistance can be used to represent a deteriorating structural system. More specifically, Straub and Der Kiureghian [20] use this information to emulate the effect of the n components on the system reliability by means of n equivalent Daniels systems (EDS) of the form of Fig. 1. The EDS representation is used there to compute the required component reliabilities needed to satisfy a given system reliability. Here, this idealisation is extended to consider time-variant system reliability, which is linked to a physics-based model of fatigue deterioration. The extended representation allows us to compute the updated system reliability resulting from inspections and repair actions at discrete points in time. Thus, the extended representation can be used to determine optimal combined design and integrity management strategies to mitigate fatigue failures for components with given importance within a system.

The EDS model of a component i consists of k independent and statistically identical Daniels systems in series, see Fig. 1. A Daniels system is a system composed of statistically identical elements in parallel that are equally loaded [23,24]. The k Daniels systems of an EDS have n_i elements and are subject to i.i.d. extreme annual loads L_j, with $j = 1, 2, \ldots, k$. The EDS elements have i.i.d. ultimate resistances $R_{j,l}$, with $l = 1, 2, \ldots, n_i$. As discussed in [20], the parameter n_i represents the redundancy of the structural system with respect to failure of component i; while k provides information about the total number of deteriorating components. By varying n_i and k, the EDS serves as a proxy for structural components with varying importance in systems of different sizes.

The calibration of the EDS representation is elaborated hereafter. The determination of the probability distribution of L_j and $R_{j,l}$ is presented in Section 2.1.1. The procedure to obtain the parameters n_i and k is explained in Section 2.1.2. The estimation of the annual probability of system failure of the EDS is elaborated in Section 2.1.3. Furthermore, the ability of the EDS idealisation to capture the behaviour of structural systems is studied with a case study in Appendix, which shows that the estimated system reliability obtained from the idealisation is sufficiently accurate to be used for reliability- and risk-based design.

2.1.1. Computation of L_j and $R_{j,l}$

The loads L_j and resistances $R_{j,l}$ of an EDS represent the characteristics of the dominant load on the true structure and its global ultimate capacity, respectively. For that purpose, they are modelled with the same distribution type and coefficient of variation as per the true structure. Let μ_{R_i} be the mean of $R_{j,l}$ and μ_L be the mean of L_j for the EDS of component i. The ratio $\mu_{R_i} n_i/\mu_L$ is obtained iteratively from the condition that the annual reliability index of the undamaged EDS $\beta'_{\bar{D}S}$ is equal to that of the true undamaged structure, i.e., $\beta_{\bar{D}S}$ in Eq. (2):

$$\beta'_{\bar{D}S} = -\Phi^{-1}\left(1 - [1 - \Pr(C|N_F = 0)]^k\right) = \beta_{\bar{D}S}, \quad (3)$$

where C denotes the event of failure of one of the k Daniels systems and N_F is the number of elements failed due to fatigue in the same Daniels system. The relation between Eq. (3) and the load and resistance parameters of the EDS depends on the behaviour of the elements. Formulations for ideal brittle and ductile elements are shown in Straub et al. [20]. For ductile behaviour, it is

$$\Pr(C|N_F = n_F) = \Pr\left(\sum_{i=1}^{n_i - n_F} R_i - L \leq 0\right), \quad (4)$$

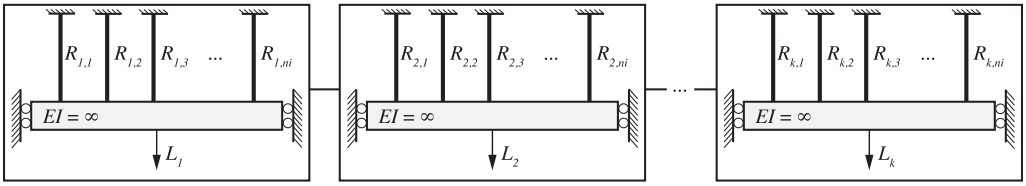

Fig. 1. The equivalent Daniels system for a component i is composed of k statistically identical and serially connected Daniels systems, which consist of n_i elements with capacities $R_{j,l}$ ($j \in [1,k], l \in [1,n_i]$) that are uniformly loaded by L_j.
Source: Figure adapted from [20].

where R_i and L have the distributions of $R_{j,l}$ and L_j, respectively, for the EDS of component i.

It is worth noticing that the assumptions on the material behaviour are not critical provided that the load and resistance variables are calibrated to a certain system reliability [20].

2.1.2. Computation of n_i and k

The parameter n_i is a measure of the importance of component i within the real structure and therefore, of the redundancy of the structure given failure of component i. The parameter n_i is computed from the condition that the EDS elements must have the same single element importance SEI_i of the corresponding component of the true structure. The conditional probability of the true system given failure of component i needed to assess SEI_i from Eq. (1) can be computed from pushover analysis, as explained in [8]. The SEI of an EDS element is computed noting that all elements of a given EDS are equally important and that the failures of the different Daniels systems are statistically independent. The following expression can then be employed to compute n_i

$$SEI_i = 1 - [1 - \Pr(C|N_F = 0)]^{k-1}[1 - \Pr(C|N_F = 1)] - \Phi(-\beta_{\bar{D}S}), \tag{5}$$

where the conditional probabilities $\Pr(C|N_F = 0)$ and $\Pr(C|N_F = 1)$ are related to n_i depending on the material behaviour, as explained in Section 2.1.1.

The parameter k is computed as the aggregate of the contributions of the EDS elements in their respective systems:

$$k = \sum_{i=1}^{n} \frac{1}{n_i}. \tag{6}$$

It follows from this equation that larger n leads to larger k for constant n_i, with $i = 1, \dots, n$. Thus, this parameter indirectly accounts for the number of deteriorating components of the true system.

The parameters n_i, k, L_j and $R_{j,l}$ of the EDS representation are iteratively computed according to the algorithm in [20].

2.1.3. Probability of failure of the EDS

A simplified model to compute the annual probability of system failure is here regarded. On a system level, the integrity of any component i is represented by a binary process with possible states: failed $F_i(t)$ or not failed $\bar{F}_i(t)$. This implies that the integrity of the structure is intact until any of its components fails. This simplification is acceptable for systems subject to high-cycle fatigue for which structural collapse is mainly driven by an extreme weather event [20], such as offshore structures subject to cyclic wave loading. For a system with n components, the deterioration state of the structure can then be determined by a process $\Psi(t)$, which may take one of the 2^n possible deterioration states, ranging from the undamaged state, $\psi_1 = \{\bigcap_{i=1}^{n} \bar{F}_i\}$, to the state with all components failed, $\psi_{2^n} = \{\bigcap_{i=1}^{n} F_i\}$, including all intermediate combinations. Let $F^*_{sys}(t)$ be the interval failure event, defined as the event of system failure in $(t-1, t]$ [25]. The interval failure probability of the system $\Pr(F^*_{sys}(t))$ is given by the total probability theorem:

$$\Pr\left(F^*_{sys}(t)\right) = \sum_{p=1}^{2^n} \Pr\left(F_{sys}|\psi_p\right) \Pr\left(\Psi(t) = \psi_p\right). \tag{7}$$

For an EDS with $n_i k$ elements, the number of unique deterioration states is lower than $2^{n_i k}$, because all of its elements are statistically interchangeable. Hence, a more convenient way of specifying a deterioration state of an EDS, denoted $\Psi' = \psi'_p$, is by the number of failed elements in each Daniels system $N_{F,j}, j = 1, 2, \dots, k$. The outcome space of Ψ' contains $(n_i + 1)^k$ distinct states, ranging from $\psi'_1 = \{N_{F,1} = 0, \dots, N_{F,k} = 0\}$ to $\psi'_{(n_i+1)^k} = \{N_{F,1} = n_i, \dots, N_{F,k} = n_i\}$. For a given deterioration state, the conditional probability of failure of the EDS is computed as

$$\Pr\left(F_{sys}|\psi'_p\right) = 1 - \prod_{j=1}^{k}\left[1 - \Pr\left(C_j|N_{F,j}(\psi'_p)\right)\right], \tag{8}$$

where C_j is the event of failure of the jth Daniels system. The conditional probability of failure of the jth Daniels system can be computed using Eq. (4).

The probability of occurrence of a certain deterioration state, i.e., $\Pr(\Psi(t) = \psi_p)$, depends on the deterioration condition of the components. Let $\boldsymbol{a}(t)$ be a vector that collects the fatigue conditions of the components of the system of interest: $\boldsymbol{a}(t) = \{a_1(t), a_2(t), \dots, a_n(t)\}$. The fatigue condition of the components can be expressed by their crack lengths and their integrity can be evaluated by a fracture-mechanics limit state function, as explained below in Section 3.2. The probability of the system taking a certain deterioration state is then given by

$$\Pr(\Psi(t) = \psi_p) = \int_{\boldsymbol{a}(t)} \psi(\boldsymbol{a}(t)) f_A(\boldsymbol{a}(t)) \mathbf{d}\boldsymbol{a}(t), \tag{9}$$

where $f_A(\boldsymbol{a}(t))$ is the joint probability density function of the crack lengths for all hot spots, and $\psi(\boldsymbol{a}(t))$ is a map between the crack lengths of the components and their integrity.

After the interval probability of failure is obtained from Eqs. (7)–(9), the cumulative probability of failure $\Pr(F_{sys,cum}(t))$ is computed to represent the history leading up to time t [25]. The cumulative probability of failure is approximated by the upper bound, in accordance with [8], assuming that failures at different years are independent

$$\Pr(F_{sys,cum}(t)) = 1 - \prod_{\tau \in [0,t]} [1 - \Pr(F^*_{sys}(\tau))]. \tag{10}$$

The annual probability of failure at year t can now be computed as

$$\Pr(F_{sys,yr}(t)) = \Pr(F_{sys,cum}(t+1)) - \Pr(F_{sys,cum}(t)). \tag{11}$$

2.2. Risk- and reliability-based fatigue design and I&M planning

This section introduces the objective functions used to assess optimal mitigation strategies. First, the cost model is presented, followed by the risk- and the reliability-based objective functions. Lastly, the selection of a target safety level for the current study is discussed.

2.2.1. Cost model

A set of N_d alternative designs $\boldsymbol{D} = \{D_1, D_2, \dots, D_{N_d}\}$ and a set of N_s I&M strategies $\boldsymbol{S} = \{S_1, S_2, \dots, S_{N_s}\}$ are considered. In this study, a design D_d consists of the specification of the FDF of the components of the system; and a strategy S_s is characterised by the specified time-interval between inspection campaigns Δt_I and the decision rule that any detected damage is subsequently repaired. A combination of D_d

and S_s defines an integrated life-cycle mitigation strategy (ILMS). For a given ILMS, the expected total life-cycle cost $\mathbb{E}[C_T]$ is the sum of the design cost C_D, the expected cost of inspection and maintenance $\mathbb{E}[C_{I\&M}]$ and the expected cost of failure $\mathbb{E}[C_F]$:

$$\mathbb{E}[C_T(\mathcal{D}_d, S_s)] = C_D(\mathcal{D}_d) + \mathbb{E}[C_{I\&M}(\mathcal{D}_d, S_s)] + \mathbb{E}[C_F(\mathcal{D}_d, S_s)], \tag{12}$$

where $\mathbb{E}[\cdot]$ is the expectation operator.

The three cost terms are elaborated hereafter:

- The design cost $C_D(\mathcal{D}_d)$ is the cost associated with designing and constructing the structural components for fatigue given a design specification $\mathcal{D}_d$. The cost associated with constructing a component with a given FDF depends on the fatigue stresses that the component is subject to. Consequently, for indeterminate systems, the design cost depends on the configuration of the structural system and the nominal cross-sections of the members [8].
- The expected inspection and maintenance cost $\mathbb{E}[C_{I\&M}(\mathcal{D}_d, S_s)]$ is the net present value cost of conducting an I&M strategy S_s for a given design $\mathcal{D}_d$. It is computed as the sum of the discounted costs of starting an inspection campaign C_C, conducting individual inspections C_I and repairing the fatigue damage C_R:

$$\mathbb{E}[C_{I\&M}(\mathcal{D}_d, S_s)] = \mathbb{E}[C_C(S_s)] + \mathbb{E}[C_I(S_s)] + \mathbb{E}[C_R(\mathcal{D}_d, S_s)]. \tag{13}$$

  Discounting of the costs is applied at the time of intervention using an interest rate r and the discount function $\gamma(t)$:

$$\gamma(t) = \frac{1}{(1+r)^t}. \tag{14}$$

- The expected cost of failure $\mathbb{E}[C_F(\mathcal{D}_d, S_s)]$, also known as the failure risk, is given by

$$\mathbb{E}[C_F(\mathcal{D}_d, S_s)] = \sum_{t=1}^{T_{SL}} C_F \cdot \gamma(t) \cdot \Pr\left(F_{sys,yr}(\mathcal{D}_d, S_s; t)\right), \tag{15}$$

  where C_F is the cost of system failure and $\Pr(F_{sys,yr}(\mathcal{D}_d, S_s; t))$ is the annual probability of system failure between years t and $t+1$ associated with $\mathcal{D}_d$ and S_s.

2.2.2. Risk-based design

The optimal risk-based ILMS is given by the minimisation of the expected total cost, which is defined in Eq. (12), i.e.,

$$\{\mathcal{D}_{opt}, S_{opt}\} = \underset{\substack{s=1,\dots,N_s;\\ d=1,\dots,N_d}}{\arg\min}\{\mathbb{E}[C_T(\mathcal{D}_d, S_s)]\}. \tag{16}$$

The minimisation of the expected life-cycle cost in Eq. (16) is sequentially assessed according to [8]:

Let $\mathbb{E}[C_{IMF}(\mathcal{D}_d, S_s)]$ denote the inspection, maintenance and failure (IMF) cost, defined as

$$\mathbb{E}[C_{IMF}(\mathcal{D}_d, S_s)] = \mathbb{E}[C_{I\&M}(\mathcal{D}_d, S_s)] + \mathbb{E}[C_F(\mathcal{D}_d, S_s)]. \tag{17}$$

Given a certain design specification $\mathcal{D}_d$, the optimal I&M strategy $S_{opt,d}$ can be obtained by minimising the expected IMF cost:

$$S_{opt,d} = S_{opt}|\mathcal{D}_d = \underset{s=1,\dots,N_s}{\arg\min}\{\mathbb{E}[C_{IMF}(\mathcal{D}_d, S_s)]\}. \tag{18}$$

This optimisation is a well established problem and the subject of many investigations, see e.g., [26–28].

The optimal ILMS $\{\mathcal{D}_{opt} \in \boldsymbol{\mathcal{D}}, S_{opt} \in \boldsymbol{S}_{opt}\}$, where $\boldsymbol{S}_{opt}$ is the vector $\boldsymbol{S}_{opt} = \{S_{opt,1}, S_{opt,2}, \dots, S_{opt,N_d}\}$, is then computed as

$$\{\mathcal{D}_{opt}, S_{opt}\} = \underset{d=1,\dots,N_d}{\arg\min}\{\mathbb{E}[C_T(\mathcal{D}_d, S_{opt,d})]\}. \tag{19}$$

2.2.3. Reliability-based design

A target annual reliability index on the deteriorated structural system is introduced, denoted β_{DS}^T. An ILMS is considered acceptable if at all times during the service life $\beta_{DS} > \beta_{DS}^T$. Two ways of performing the reliability-based design are considered.

1. The minimum requirements for one of the decision parameters can be prescribed as a function of the other. Finding the minimum acceptable decision parameter becomes a minimisation problem when a discretised set of the parameter is considered. In the following, we focus on the more intuitive case of a maximum allowed inspection interval $\Delta t_{I,max}$ for a given FDF. Let β_{DS}^{min} denote the minimum reliability index during service life, i.e., $\beta_{DS}^{min} = \min_{t=0,1,\dots,T_{SL}}\{\beta_{DS}(t)\}$. The maximum allowed inspection interval is estimated as

$$\begin{aligned} S_{min}|\mathcal{D}_d = \Delta t_{I,max}(FDF) = \underset{s=1,\dots,N_s}{\arg\min}\left[\beta_{DS}^{min}(S_s, \mathcal{D}_d) - \beta_{DS}^T\right], \\ \text{s.t. } \beta_{DS}^{min}(S_s, \mathcal{D}_d) > \beta_{DS}^T. \end{aligned} \tag{20}$$

2. The optimal reliability-based ILMS is defined as the one that minimises the total mitigation cost $C_{T,M}$, while satisfying the target reliability:

$$\begin{aligned} \{\mathcal{D}_{opt}, S_{opt}\} = \underset{\substack{s=1,\dots,N_s;\\ d=1,\dots,N_d}}{\arg\min}\left[C_{T,M}(\mathcal{D}_d, S_s)\right], \\ \text{s.t. } \beta_{DS}^{min}(S_s, \mathcal{D}_d) > \beta_{DS}^T. \end{aligned} \tag{21}$$

   The total mitigation cost $C_{T,M}$ is defined as the sum of the design and expected inspection and maintenance cost:

$$C_{T,M}(\mathcal{D}_d, S_s) = C_D(\mathcal{D}_d) + \mathbb{E}[C_{I\&M}(\mathcal{D}_d, S_s)], \tag{22}$$

   where $\mathbb{E}[C_{I\&M}(\mathcal{D}_d, S_s)]$ is defined in Eq. (13).

2.2.4. Selection of the target safety level

Institutions such as the International Organization for Standardization (ISO) and the Joint Committee on Structural Safety (JCSS) prescribe target safety levels in the form of target reliability indices β^T [29,30]. According to this criterion, a component or structure is considered acceptable if its reliability index is larger than β^T. For instance, JCSS's Probabilistic Model Code specifies ULS target reliability indices for nine different classes. Classes are specified according to the consequence of component failure (minor, moderate and large) and the relative cost of the safety measure (small, normal and large). The adoption of this classification in the current study is discussed in the following.

The consequences of component failure are, for a given cost of system failure, explicitly represented in the proposed system idealisation by the parameter n_i. The classification according to the relative cost of the safety measure does not accommodate for the simultaneous consideration of two different safety measures. Pragmatically, one can regard the most effective safety measure for categorisation.

In the current study, two different ULS are considered: ultimate load limit state (STR) and fatigue limit state (FLS). Structural reliability for STR is measured by the reliability index of the undamaged system $\beta_{\bar{D}S}$. The reliability during service life is measured by the reliability index of the damaged system β_{DS}. During service life, the reliability of the structure decreases over time due to deterioration if no actions are taken, i.e., $\beta_{DS} \leq \beta_{\bar{D}S}$. The reliability index of the damaged system relates to both STR and FLS. It is unclear whether the prescribed target reliability values in [29–31] refer to the undamaged or the damaged system, i.e., if they are a direct constraint to $\beta_{\bar{D}S}$ or β_{DS}. On the one hand, applying the requirement to $\beta_{\bar{D}S}$, i.e., $\beta_{\bar{D}S}^T = \beta^T$, requires to specify an additional annual target reliability index for the deteriorated system β_{DS}^T, with $\beta_{DS}^T \leq \beta^T$. On the other hand, applying it to β_{DS}, i.e., $\beta_{DS}^T = \beta^T$, would leave $\beta_{\bar{D}S}$ as another degree of freedom of the optimisation problem. The latter interpretation would greatly increase the complexity of the problem.

Typically, standards and recommended practice guidelines separately prescribe required safety levels for FLS and STR. For example, the Eurocode 0 [31] requires a 50-year cumulative reliability index for FLS in the range 1.5 to 3.8 depending on the "degree of inspectability, repairability and damage tolerance". Similarly, DNV [4] requires a 20-year cumulative reliability index for FLS between 2.3 and 3.7, depending on the consequences of component failure. This separate prescription of target reliabilities for FLS strengthens the argument that the prescribed levels for ULS refer to the undamaged system. Accordingly, we follow this interpretation and adopt the criterion $\beta_{\bar{D}S} > \beta^T$. We use the annual target $\beta^T = 4.2$ in the numerical investigation, since it is associated with the most common design class in ISO 2394:2015 [29] and JCSS [30]. Additionally, the target reliability index of the deteriorated system β^T_{DS} is set to a value relatively close to β^T. We choose $\beta^T_{DS} = 4$, which is approximately 5% lower than $\beta^T = 4.2$ and that corresponds to the target reliability index set for offshore structures in ISO 19902:2020 [3,32].

3. Characteristics of the numerical investigation

A parametric study is conducted over the parameters n_i and k of the EDS representation to find how the ILMS varies with n_i and k. Optimal ILMS is assessed by exhaustive search, i.e., by evaluating the system reliability and the expected total life-cycle cost for all considered ILMS. Despite the availability of more efficient optimisation algorithms, the use of exhaustive search is preferable for the current application. This is due to the fact that risk- and reliability-based optimal ILMS depend on the cost model. Consequently, systematically evaluating all ILMS allows to efficiently compute the optimum for any cost model by appropriately scaling the results. This is convenient in the context of standardisation, where prescriptions are given as a function of the relative cost of the safety measures and the consequence class.

The optimisation searches within a discrete set of $N_d = 7$ designs $\boldsymbol{D}$ associated with $FDF = \{1, 2, 3, 4, 5, 6, 10\}$. These values cover the typical range in design standards [33]. Note that $FDF = 10$ is often prescribed for non-accessible hot spots [1]. All $n_i k$ elements are assigned the same FDF. A set of $N_s = 11$ strategies $\boldsymbol{S}$ are considered, given by the inspection intervals between inspection campaigns $\Delta t_I = \{1, 2, \ldots, 10\}$ [years], plus the case with no inspections, here denoted NI. All $n_i k$ EDS elements are inspected at every inspection campaign and, as simplifying convention, every detected fatigue crack is subsequently repaired. Repairs are assumed to restore the fatigue condition to as-new, i.e., that of a component at time zero.

For each considered structural configuration and combination of life-cycle mitigation measures, the annual probability of failure of the EDS is computed using the sampling-based method proposed in [28]. It is noted that this method is computationally expensive. For each design situation, 250 deterioration histories are sampled. In our implementation in Matlab, this requires an average of around 35 s per component by using the processor Intel Xeon Gold 6132. Thus, in order to remain computationally feasible, the scope of the parametric study needs to be carefully specified in terms of the discretisation of the decision variables as well as the considered combinations of n_i and k.

In order to choose the range of considered n_i and k, their effect on the SEI' is assessed. Fig. 2 shows the SEI' of EDS elements for varying n_i and k, which is computed using Eq. (5). Increasing n_i from 1, i.e., no redundancy or $SEI' \approx 1$, to say 5 reduces the SEI' noticeably. Further increasing n_i has a smaller impact on the SEI'. Increasing k, which is associated with the size of the true structure, also results in a reduction of the SEI', although its impact is overall less important than that of n_i. For these reasons, the parametric study presented in this article is constrained to $n_i \in [1, 5]$ and $k \in [1, 6]$. The considered combinations of n_i and k are shown in Fig. 3. Thus, the total number of simulations is $23 \cdot 7 \cdot (10 \cdot 250 + 1) = 402661$.

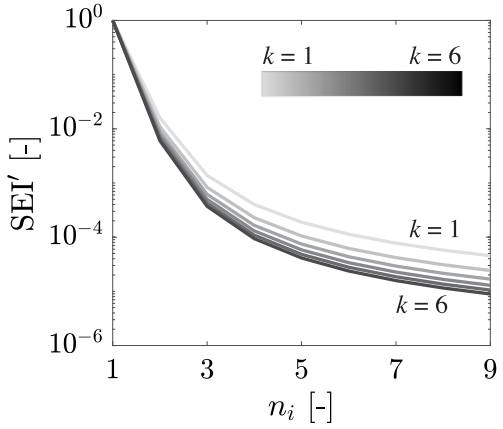

Fig. 2. Single element importance SEI' as a function of the equivalent Daniels system parameters n_i and k for a reliability index of the intact structure $\beta_{\bar{D}S} = 4.2$.

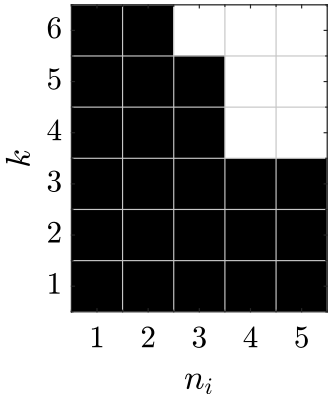

Fig. 3. Considered combinations of n_i and k.

3.1. Probabilistic load and resistance model

The probabilistic model of the load and resistance variables is chosen to be representative for offshore platforms. Nonetheless, the proposed method can accommodate for the use of any other probabilistic models. The $n_i k$ EDS elements are assumed to have ductile material behaviour, with log-normal distributed resistances R. The coefficient of variation of R is taken as $\delta_R = 0.15$, which is a representative value according to [34,35]. The loads on the Daniels systems L is represented with a Gumbel distribution with coefficient of variation $\delta_L = 0.35$. The probabilistic model of R and L is calibrated, as explained in Section 2.1.1, to an annual reliability of the undamaged system $\beta_{\bar{D}S} = 4.2$.

3.2. Fatigue component reliability

A stochastic physics-based model is used to assess the fatigue deterioration process. For a given hot spot, the crack length is used as a physical indicator of fatigue deterioration. The crack length of a hot spot is predicted using a fracture mechanics model based on prior information. A brief description of the employed crack growth model is here presented. The parameters and assumptions of the model are described in more detail in [8]. The crack length of a hot spot at time t is given by

$$a(t) = \left[\left(1 - \frac{m}{2}\right) \cdot C \cdot \Delta S_e^m \cdot \pi^{m/2} \cdot \nu \cdot t + a_0^{(1-m/2)}\right]^{(1-m/2)^{-1}}, \tag{23}$$

where C and m are material parameters, ν is the number of stress cycles per year, a_0 is the initial crack length, and ΔS_e is the equivalent

Table 1
Distribution of the variables of the fatigue deterioration model.

Variable	Type	Mean	Standard deviation
a_0	Exponential	1 mm	1 mm
m	Normal	3.5	0.3
$\ln k_{\Delta S}{}^*$	Normal	$f(FDF)$	0.22
λ	Deterministic	0.8	–
a_{cr}	Deterministic	10 mm	–
ν	Deterministic	10^5 cycles/year	–
T_{SL}	Deterministic	20 years	–

Notes: ${}^*k_{\Delta S}$ has units of N/mm^2; $f(FDF)$ = function of FDF.

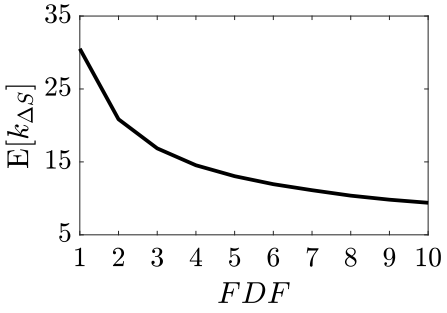

Fig. 4. Calibrated mean value of the stress range Weibull parameter $k_{\Delta S}$ as a function of the fatigue design factor FDF.

fatigue stress range, which represents the stress process. The values of the deterioration parameters are shown in Table 1. The parameter C is computed as $\ln C = -1.567m - 27.517$, according to Bismut et al. [36].

The fatigue stress process $\Delta S(t)$ is assumed to be represented by a Weibull distribution with scale parameter $k_{\Delta S}$ and shape parameter λ. The equivalent stress range ΔS_e is then given by

$$\Delta S_e = \mathbb{E}[\Delta S(t)^m]^{(1/m)} = k_{\Delta S} \cdot \Gamma\left(1 + \frac{m}{\lambda}\right)^{(1/m)}, \tag{24}$$

where $\Gamma(\cdot)$ is the gamma function.

The fatigue reliability of a component is assessed according to the limit state function

$$g_c(t) = a_{cr} - a(t), \tag{25}$$

which indicates component failure $g_c \leq 0$ if the crack length a reaches a critical magnitude a_{cr}.

Increasing the FDF of a hot spot decreases the fatigue stress range that it experiences. This is accounted for in the model by calibrating the mean value of the shape parameter $k_{\Delta S}$ so that the cumulative probability of fatigue failure of the component at the end of service life correctly represents its FDF [8], see Fig. 4. It is assumed that the global response of the structure is independent of the FDF of the components. This assumption should be verified on a case-by-case basis, specially for very low and very high values of the FDF.

The parameters a_0, m and $k_{\Delta S}$ are statistically dependent among the different hot spots. These dependencies are represented by the following assumed linear correlation coefficients: $\rho_{A_0} = 0.5$, $\rho_M = 0.6$ and $\rho_{K_{\Delta S}} = 0.8$ for a_0, m and $k_{\Delta S}$, respectively. The statistical dependence is efficiently represented by the hierarchical Bayesian Network developed by Luque et al. [37].

3.3. Likelihood model of the inspection technique

Inspections can be conducted during the service life of the structure. The outcomes of these inspections are imperfect, meaning that cracks are not identified with absolute certainty. The employed likelihood functions that are used to model the quality of the inspections are taken after [38]. The probability of detection (PoD) curve that is used to assess the likelihood of detecting a crack with length a is:

$$PoD(a) = 1 - \exp(-a/\xi), \tag{26}$$

where ξ is the expected minimum crack that can be detected. ξ is set to 10 mm, which corresponds to a relatively unreliable inspection technique, such as visual inspections.

Furthermore, detected cracks are imperfectly measured. The measurement of a crack, denoted z, is modelled by the following likelihood function:

$$f_{Z|a}(z|a) = PoD(a) \cdot \frac{\varphi\left(\frac{z-a}{\sigma_\varepsilon}\right)}{1 - \Phi\left(\frac{-a}{\sigma_\varepsilon}\right)} \quad \text{for } z > 0, \tag{27}$$

where $\sigma_\varepsilon = 0.1$ mm is the measurement error and $\varphi(\cdot)$ is the probability density function of the standard normal distribution. The information of the measurement of the crack length is propagated to the rest of the hot spots of the system applying inference using the hierarchical Bayesian Network.

3.4. System reliability

The system reliability is assessed according to an ultimate load limit state. The probability of failure of the system conditional on a deterioration state $\Pr\left(F_{sys}|\psi'_p\right)$, defined in Eq. (8), can be pre-computed for the different $(n_i+1)^k$ deterioration states. It is assumed that the EDS elements are ductile and thus, the term $\Pr(C_j|N_{F,j})$ in that equation is computed using Eq. (4). It is noted that modelling the behaviour as brittle would not lead to significantly different conclusions, since the EDS is calibrated to a given system reliability.

As previously shown, the reliability of the system is time-dependent and is influenced by the deterioration condition of the components. A Bayesian Network (BN) is used to represent the causal structure between mitigation measures of fatigue deterioration at the component level and the system reliability. The employed BN is proposed in [8] and based on original work in [28,37,38]. The reader can refer to these publications for further information.

The annual probability of failure $\Pr(F_{sys,yr}(t))$ is computed from Eq. (11) as explained in Section 2.1.3. In addition to the annual probability of failure, we introduce the hazard function $h(t)$, which is defined as the probability of system failure during $(t, t+1]$ conditional on the system not having failed up to time-step t. The hazard function is expressed mathematically as

$$h(t) = \frac{\Pr(F_{sys,yr}(t))}{1 - \Pr(F_{sys,cum}(t))}. \tag{28}$$

The difference between the hazard function and the annual probability of failure is illustrated in Fig. 5. It can be seen that both $\Pr(F_{sys,yr}(t))$ and $h(t)$ are practically identical when the cumulative probability of failure is low, which is the case during the initial service years. The difference between the two probabilities increases as the system deteriorates, and is large for cases with low fatigue reliability, say $FDF < 3$. In fact, the annual probability of failure starts decreasing after a number of service years for $FDF < 3$, because the cumulative probability of failure asymptotically approaches unity and therefore, the rate at which it increases between two subsequent time steps decreases. Because the annual probability of failure is not necessarily monotonically increasing during the service life of the structure, we use the hazard rate to estimate the annual reliability index of the deteriorated structural system $\beta_{DS}(t)$ in this paper:

$$\beta_{DS}(t) = -\Phi^{-1}\left[h(t)\right]. \tag{29}$$

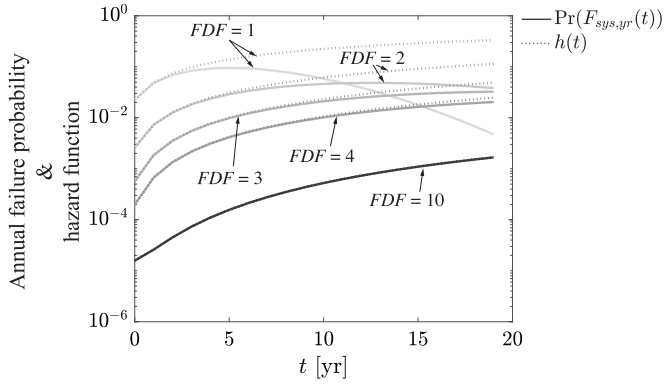

Fig. 5. Time evolution of the annual probability of system failure $\Pr(F_{sys,yr}(t))$ and hazard function $h(t)$ with no inspections for $k = 2$ and $n_i = 1$.

Table 2
Unitary cost input of reference cost model.

Cost	Symbol	Value
Inspection campaign	c_C	1 k€
Inspection 1 component	c_I	0.1 k€
Repair 1 component	c_R	0.3 k€
System failure	c_F	1,000 k€
Discount rate	r	0.02
Cost per kg of steel	c_s	6 €

3.5. Cost input

The cost model has a large impact on the optimality of decisions. Here, the expected life-cycle cost is linearly proportional to the expected values of the different unitary costs model. Therefore, translating the results to different situations is a matter of accordingly scaling the different costs. The employed unitary cost model is shown in Table 2. The unitary costs of inspection and repair actions are adopted after [28], which uses them to represent an offshore structure. The fatigue design cost is computed according to the model proposed in [8], which is developed for structures consisting of tubular members. In that model, the cross-section area of a hot spot, denoted A_{HS}, is expressed as a function of the mean equivalent fatigue stress range $\mathbb{E}[\Delta S_e]$ and the equivalent internal fatigue load range ΔN_e

$$A_{HS}(FDF) = \frac{\Delta N_e}{\mathbb{E}[\Delta S_e]} = \frac{\Delta N_e}{\mathbb{E}[k_{\Delta S}] \cdot \mathbb{E}\left[\Gamma\left(1 + \frac{m}{\lambda}\right)^{(1/m)}\right]}, \tag{30}$$

The parameter $\mathbb{E}[k_{\Delta S}]$ is a function of the FDF, as specified in Fig. 4. Consequently, the fatigue design cost of a hot spot, denoted C_{HS}, is also a function of the FDF and is estimated as

$$C_{HS} = \frac{3\pi}{2} \rho_s \cdot c_s \cdot A_{HS}^{3/2}, \tag{31}$$

where $\rho_s = 7850$ kg/m^3 is the density of steel and c_s is the cost of steel shown in Table 2, which includes the cost of welding.

The fatigue design cost is case dependent because it is a function of the nominal load carried by the member of interest, among other factors. Two costs models are employed here for the purpose of illustration and to study the robustness of the results with respect to the cost model (see Fig. 6): cost model C1 takes $\Delta N_e = 0.6$ MN; and cost model C2 takes $\Delta N_e = 1.25$ MN, which corresponds to a three-fold increase of the fatigue design cost associated with C1. In spite of using these two cost models, most of the presented results are independent of the fatigue design cost to strive for generalisation.

3.6. Regression model of the expected repair costs

The estimation of the expected I&M cost is associated with statistical uncertainty, which have its origin in the limited number of Monte Carlo simulations that are sampled to evaluate the stochastic deterioration process. This statistical uncertainty primarily affects the estimation of the expected repair costs. To reduce this uncertainty, a regression model of the expected repair cost is developed from all the simulated data, thereby taking advantage of the 402,661 simulations, instead of just the 250 ones that are associated with a particular EDS and a given ILMS. First, the expected number of repairs n_{rep} is calculated for each tested combination of k and n_i and as a function of the mitigation parameters from 250 samples. The probability of conducting a component repair during an inspection campaign, denoted p_{rep}, is computed as

$$p_{rep} = \frac{n_{rep}}{n_{insp,c} \cdot k \cdot n_i}. \tag{32}$$

where $n_{insp,c}$ is the number of inspection campaigns, given by

$$n_{insp,c} = \left\lfloor \frac{T_{SL} - 1}{\Delta t_I} \right\rfloor, \tag{33}$$

with $\lfloor \cdot \rfloor$ being the flooring operator.

A power-law of the form $p_{rep} = a \cdot FDF^b \cdot \Delta t_I^c$ is fitted to the simulated data. The regression parameters are computed using the maximum likelihood method, resulting in $a = 0.100$, $b = -0.385$ and $c = 0.209$. The fitted curve is shown in Fig. 7. Note that the validity of the curve is bound to $1 \leq FDF \leq 10$ and $1 \leq \Delta t_I \leq 10$. The coefficient of determination of the regression model is 0.6. This low value is partially due to the large variability in the obtained number of repairs from the numerical simulations. Nevertheless, using the model is justified since we are only interested in the average cost of repair for decision making purposes.

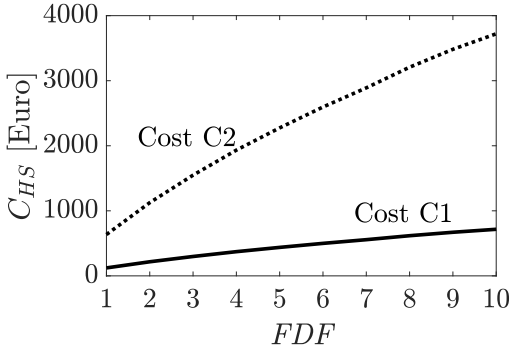

Fig. 6. Fatigue design cost C_{HS} as a function of the fatigue design factor FDF for the two costs models C1 and C2.

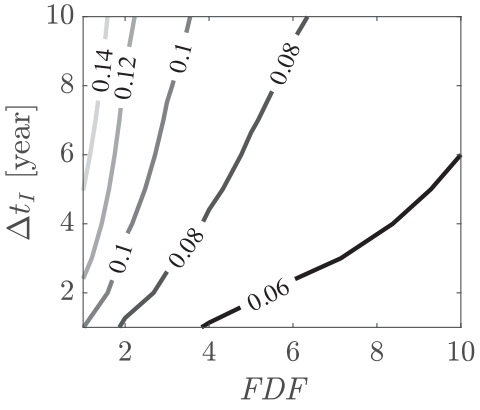

Fig. 7. Contour plot of the probability of conducting one repair p_{rep} as a function of the interval between inspection campaigns Δt_I and the fatigue design factor FDF.

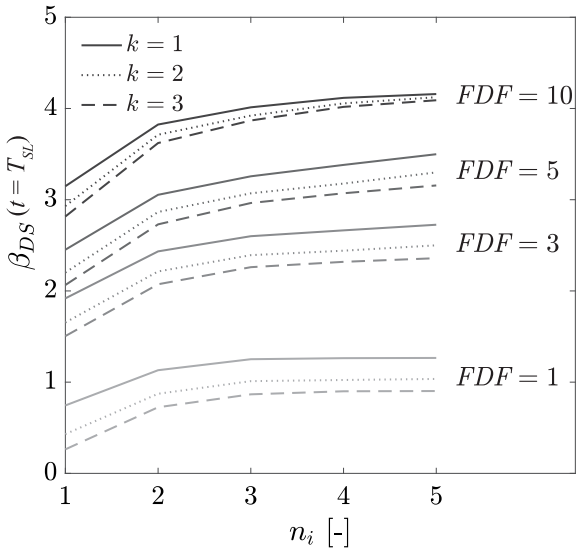

Fig. 8. Annual reliability index of the deteriorated structural system $\beta_{DS}(t = T_{SL})$ at the end of service life as a function of n_i with no conducted inspections. Plots are given for various values of k and FDF.

The expected cost of repair is then given by

$$C_R = c_R \cdot p_{rep} \cdot k \cdot n_i \sum_{j=1}^{n_{insp}} \gamma(j \cdot \Delta t_I)[1 - F_{sys,cum}(j \cdot \Delta t_I)], \tag{34}$$

where γ is the discount function defined in Eq. (14). At a given inspection time $j \cdot \Delta t_I$, the cost of repair is multiplied by the probability of survival, since a repair will only be conducted if the structure is not failed.

4. Results

The results of the parametric investigation are presented in this section. First, the results of the reliability-based study are shown in Section 4.1. The results of the risk-based optimisation are shown in Section 4.2.

4.1. Reliability-based life-cycle optimisation

Fig. 8 shows the annual reliability index at the end of service life $\beta_{DS}(t = T_{SL})$ for varying n_i, k and FDF when no inspections are conducted. It is observed that the level of redundancy, measured via n_i, is a crucial factor in assuring sufficient safety for systems that are sensitive to fatigue deterioration. Even for $FDF = 10$, no redundancy results in β_{DS} being only around 3, which is significantly lower than the undamaged reliability index $\beta_{DS} = 4.2$.

Minimum requirements for the mitigation measures are computed according to the target reliability index $\beta_{DS}^T = 4$. As an example, Fig. 9 shows which combinations of the mitigation measures satisfy this requirement for $k = 4$ and $n_i = 1, 2, 3$. The maximum acceptable inspection interval is computed as a function of the FDF according to Eq. (20). The results are displayed in Fig. 10. Note that the curves are only plotted for the situations satisfying the target reliability criterion.

Optimal reliability-based mitigation strategies are then computed according to Eq. (21). The optimal reliability-based ILMS are marked in red and blue in Fig. 10 for the cost models C1 and C2, respectively. It can be seen that an increase of a factor of three in the design cost model has a minimal impact in the optima for the employed discretisation of the design parameter. The optimal allocation of the total mitigation cost $C_{T,M}$ among the design and I&M measures is plotted for cost C1 in Fig. 11, where the expected I&M cost $\mathbb{E}[C_{I\&M}]$ is divided into the campaign C_C, inspection C_I and repair C_R costs. When the optimal ILMS is associated with very frequent inspections (see $k = 1, n_i = 1$), the total mitigation cost is driven by the I&M cost. In particular for this case, the I&M cost is largely associated with the inspection campaign cost, which is explained by (a) the campaign cost is ten times larger than the cost of inspecting one component; and (b) most inspections will lead to not detecting a crack because of the large FDF value and thereby, to not conducting many repairs. Furthermore, it is seen that for systems with large redundancy, one can afford to do without preventive inspections. For multi-components systems with some redundancy, a balance between design and I&M mitigation measures is optimal. For these cases, the optimal inspection interval is large, and as consequence, the repair cost tends to take a large share of the total mitigation cost, due to fact that the probability of detecting cracks increases.

4.2. Risk-based life-cycle optimisation

The expected life-cycle cost $\mathbb{E}[C_T]$ is computed according to Eq. (12) for the considered combinations (see Fig. 3) and plotted for $k = 1$ and $n_i = 1, 2, 5$ in Fig. 12 as a function of the inspection interval Δt_I and for the different FDF. It is observed that the expected life-cycle cost curve becomes flatter around the optimum I&M strategy for increasing FDF. It is also seen that increasing n_i eventually reduces the efficiency of increasing the FDF to reduce the life-cycle cost.

The optimal inspection interval for given FDF is summarised in Fig. 13. It is cost-efficient from a risk-based perspective to conduct

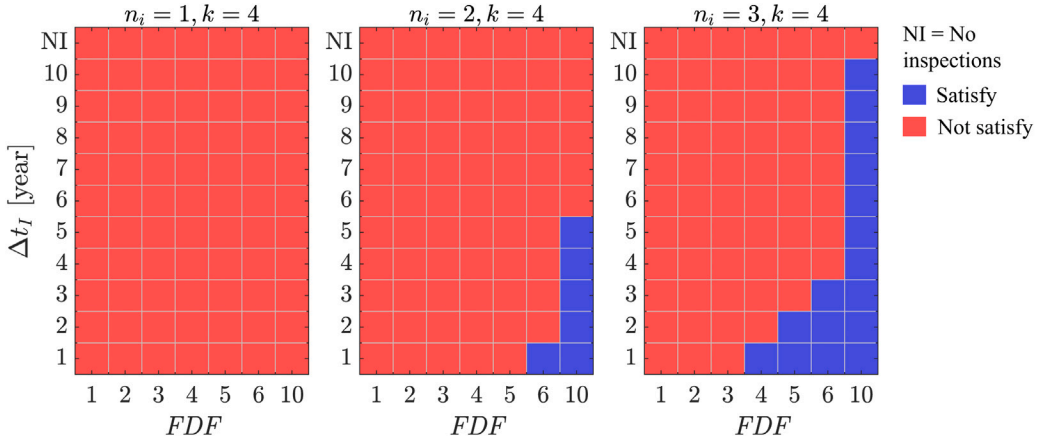

Fig. 9. Colour-map representing which combinations of the mitigation measures satisfy or not the reliability criterion given by a target reliability index of the deteriorated structure $\beta_{DS}^T = 4$, i.e., $\beta_{DS}^{min} > \beta_{DS}^T$. Note that for $n_i = 1, k = 4$ no mitigation strategy satisfy the criterion.

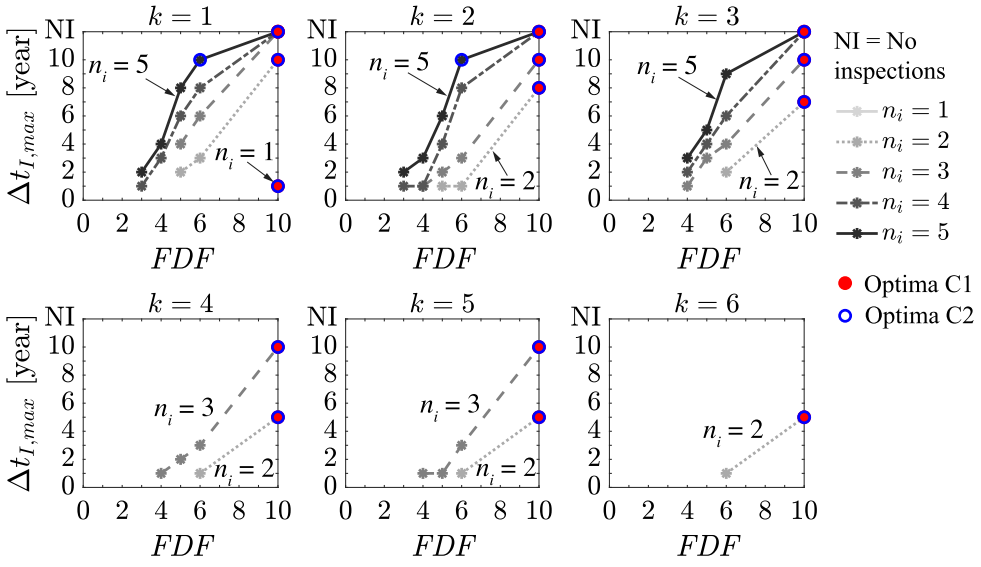

Fig. 10. Maximum acceptable inspection interval Δt_I as a function of the fatigue design factor FDF and for given k and n_i. A target reliability index of the deteriorated structure $\beta_{DS}^T = 4$ is used. The resulting combined optimal reliability-based FDF and Δt_I are marked for cost models C1 and C2.

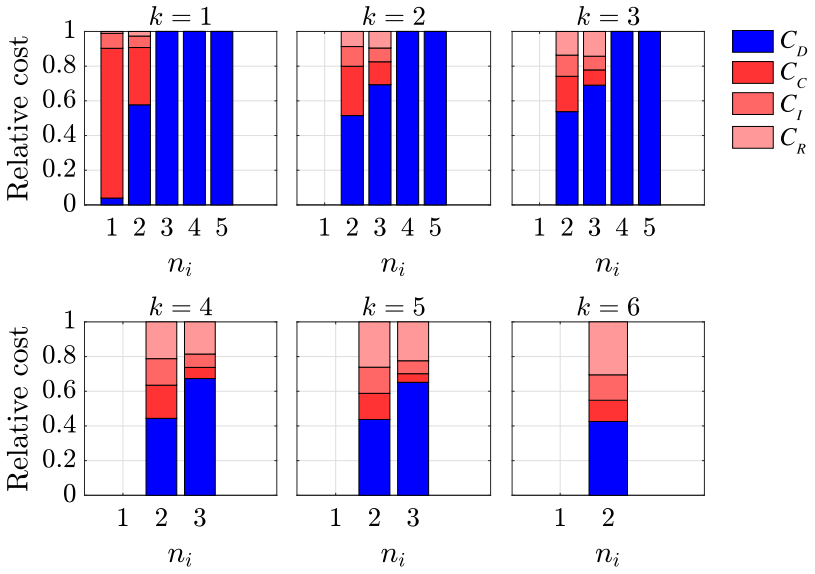

Fig. 11. Allocation of the total mitigation cost associated with the optimal reliability-based mitigation strategy for cost model C1 (marked in red in Fig. 10) among the design cost C_D and the expected inspection and maintenance cost $\mathbb{E}[C_{I\&M}]$, which is the sum of the costs of campaign C_C, inspection C_I and repair C_R. Only the mitigation strategies that satisfy the minimum reliability requirements are plotted.

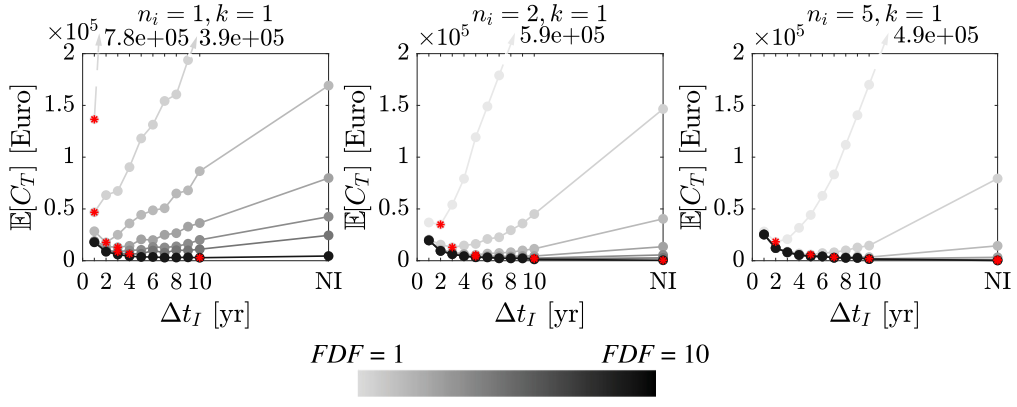

Fig. 12. Expected total life-cycle cost $\mathbb{E}[C_T]$ for different structural systems, parametrised by n_i and k, as a function of the inspection interval Δt_I. The different curves correspond from higher to lower costs to $FDF = 1, 2, 3, 4, 5, 6, 10$. Minimal expected total cost for given FDF is marked with a red dot. Note that NI refers to no inspections.

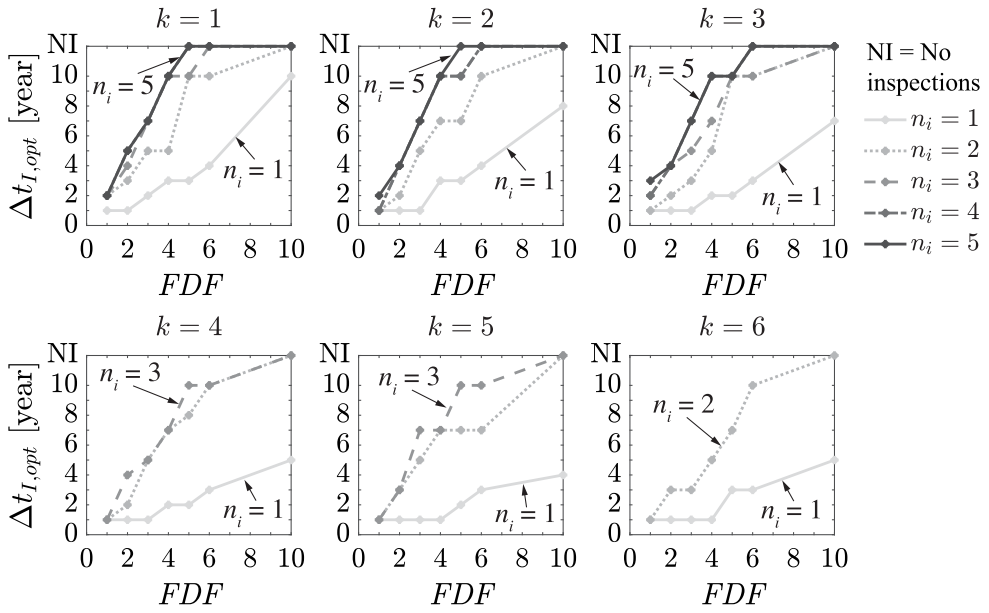

Fig. 13. Risk-based optimal inspection interval $\Delta t_{I,opt}$ as a function of the fatigue design factor FDF for all considered values of k and n_i.

inspection campaigns for systems with no redundancy ($n_i = 1$), even for components with $FDF = 10$, which indicates that it might be cost-efficient to reach larger safety levels than the ones prescribed in standards for this situation [1,4].

5. Discussion

The current fatigue design practice focuses on the specification of component design parameters and is not thoroughly preoccupied with the simultaneous prescription of the associated posterior integrity management. The fact that requirements for the I&M program are not specified for a given fatigue design suggests that one should, at later stages of the life cycle, identify and choose an I&M program that satisfies the reliability requirements. Generally, this approach leads to sub-optimal decisions. In this paper, we showed that the consideration of system effects and life-cycle mitigation alternatives at the design phase has the potential to significantly lower the expected total cost. However, additionally taking these aspects into account is computationally demanding. In this paper, we have studied patterns of optimal life-cycle mitigation strategies to provide simplified recommendations that can be followed in practice.

We use and extend the EDS representation proposed by Straub et al. [20] to idealise and differentiate structural configurations according to selected key features. The employed level of abstraction is appropriate for the purpose of standardisation and code-calibration. The obtained results can be used by code-makers for the prescription of mitigation measures at the design stage and to bring attention to the important issue of accounting for system effects for the design of deteriorating systems. Furthermore, the results of the study show the potential improvement in efficiency of fatigue mitigation associated with using structural redundancy as an additional design parameter.

The optimisation of fatigue mitigation measures has been separately conducted in accordance with reliability- and risk-based criteria, as both criteria are relevant to engineering practice. Following one criterion or the other is a choice of the designer, infrastructure owner, and operator, provided that the applicable regulations allow for such choice. In principle, reliability-based design is coherent with the risk-based criterion as long as the employed target probability of failure is calibrated by risk-based optimisation.

Minimum requirements for inspection plans to satisfy the target reliability index $\beta_{DS}^{T} = 4$ throughout the service life are studied as a function of the FDF. Fig. 10 shows that the specification of low FDF (in the range 3 to 4) is acceptable for systems with some redundancy and when accompanied by frequent inspections (every 1 to 3 years). Nevertheless, the results in Figs. 10 and 11 indicate that it is optimal to specify larger FDF at design. Therefore, for structures that are identified with the employed cost models, which can be the case for offshore structures, we recommend to design the fatigue components with high reliability ($FDF \approx 10$) and subsequently find an appropriate inspection plan.

The results in Fig. 10 also show that hot spots that cannot be inspected need to be designed with $FDF \geq 10$ and that, additionally, certain structural redundancy must be assured in order to satisfy the reliability requirements. Systems with no redundancy can only satisfy the imposed reliability requirements when there is one single deteriorating component ($k = 1$) and by specifying $FDF \geq 10$ together with a strict I&M program. This suggests that minimum requirements in most design standards are associated with lower system reliability than the target that is used in the current study, i.e., $\beta_{DS}^{T} = 4$.

Optimal risk-based I&M strategies for given design are explored in Fig. 13. It is shown that optimal risk-based ILMS are less strict than the reliability requirements discussed above. For instance, results for FDF in the range 2 to 4 are associated with a reliability index between 2.4 to 3.6, which is significantly lower than $\beta_{DS}^{T} = 4$. These results can be particularly useful for the design of unmanned structures with low consequences of failure, such as offshore wind turbines.

6. Conclusions

In this paper, the efficiency of life-cycle fatigue mitigation measures have been assessed as a function of two selected system features, namely the redundancy and the number of deteriorating components. Considered mitigation measures are the specification of the fatigue design factor for the hot spots and the fixed time-interval between inspection campaigns. Reliability-based requirements for the mitigation measures and risk-based optimal mitigation strategies have been studied within a parametric study over the system features. Results show the potential reduction of the expected total cost that can be achieved by considering life-cycle mitigation alternatives and assessing structural design from a system perspective. Based on a cost model that is representative for offshore structures, we showed that it is optimal to design the fatigue hot spots with high reliabilities (FDF

around 10) and to prescribe a corresponding inspection plan to satisfy the system reliability requirements. Furthermore, specifying $FDF = 10$ for the components of non-redundant structures is not sufficient to avoid preventive inspections. Lastly, we showed that optimal risk-based designs are associated with lower reliabilities than the optimal reliability-based designs, which can be used as arguments to lower the requirements for unmanned structures with low consequences of failure.

The results of the present study are subject to the applicability of the employed probabilistic load and resistance models. Further studies could be carried out for different probabilistic models to study how these choices affect the conclusions. Moreover, future studies could implement more sophisticated risk-acceptance criteria, such as the marginal life-saving costs criterion, to assess acceptability as a function of the expected number of fatalities given the societal budget for safety.

CRediT authorship contribution statement

Jorge Mendoza: Conceptualisation, Formal analysis, Investigation, Methodology, Visualisation, Validation, Software, Writing – original draft, Writing – review & editing. **Elizabeth Bismut:** Software, Validation, Writing – review & editing. **Daniel Straub:** Conceptualisation, Funding acquisition, Methodology, Software, Supervision, Writing – review & editing. **Jochen Köhler:** Conceptualisation, Methodology, Supervision, Writing – review & editing.

Declaration of competing interest

The authors declare that they have no known competing financial interests or personal relationships that could have appeared to influence the work reported in this paper.

Acknowledgements

The computations were performed on resources provided by the NTNU IDUN/EPIC computing cluster [39]. Elizabeth Bismut and Daniel Straub acknowledge the support by Deutsche Forschungsgemeinschaft (DFG) through the TUM International Graduate School of Science and Engineering (IGSSE).

Appendix. Model validation

The EDS representation was shown in [20] to perform well for the calibration of the reliability index of deteriorating components given safety level requirements for the system. In that case, the deterioration condition was represented by a random variable with two states: "failed" and "safe". As a consequence, the deterioration process leading to failure of the components was neglected. To assess optimal inspection planning, the evolution of an observable indicator, such as the fatigue cracks, needs to be explicitly considered. We present in this section a validation example to evaluate the performance of the EDS representation in comparison to the assessment of the complete structural system (CSS).

Exemplary, the lattice structure in Fig. A.14 is considered. This structure is analysed in detail in [8]. It consists of six tubular members connected by welded joints and a horizontal, rigid beam at the top. The structure is redundant with respect to single member failure. The structure is subject to an extreme environmental load with annual maximum Q, which is represented by a Gumbel distribution with coefficient of variation $\delta_Q = 0.35$. The resistance of the structural members is assumed to be deterministic. The reliability index of the undamaged structure is $\beta_{\bar{D}S} = 4.6$. In addition to the extreme environmental loading, the structure is subject to cyclic loading. Four hot spots (HS1–HS4) are identified near the welded connections, see Fig. A.14. It is assumed that the remaining connections have a sufficiently large reliability and are not sensitive to fatigue failure. The four hot spots are associated

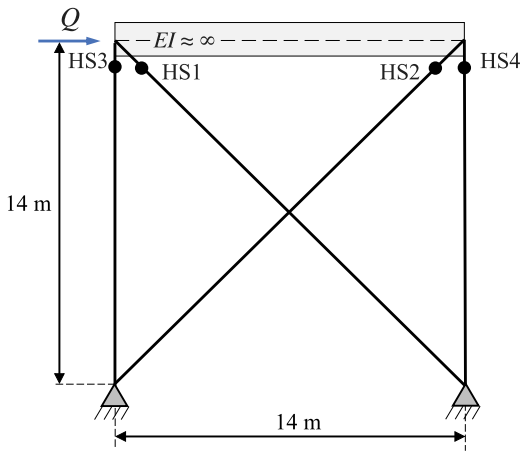

Fig. A.14. Structure used for the validation example of the equivalent Daniels system representation.
Source: Edited from [8].

with $SEI = 0.0030$. The cyclic load induces fatigue stress ranges $\Delta S_i(t)$ at the hot spots. $\Delta S_i(t)$ is represented by a Weibull distributed process with shape parameter $k_{w,i}$ and λ_w, as per the parametric study above.

The validation example is conducted for two situations: (1) all hot spots have $FDF = 5$, and (2) all hot spots have $FDF = 10$. The fatigue integrity of the hot spots is assessed using a critical crack depth $a_c = 10$ mm. The parameters n_i and k of the EDS representation are calculated as explained above, see Eqs. (5) and (6), resulting in $n_i = 2$ and $k = 2$ for all components.

A.1. Accuracy of the reliability estimation

The error in the estimation of the annual reliability index of the deteriorating system β_{DS} is investigated. This reliability index is computed as explained in Section 2.1.3. Eq. (7) is used to compute the interval failure probability, which requires summing over $2^4 = 16$ deterioration states for the CSS and over $(2+1)^2 = 9$ deterioration states for the EDS. The probability of system failure conditional on the deterioration state is computed from pushover analysis for the true structure and Eq. (8) is used for the EDS. For both the CSS and the EDS, Eqs. (10) and (11) are used to compute the annual probability of system failure. The annual reliability index β_{DS} is computed from the hazard function, see Eqs. (28) and (29). The results are shown in Fig. A.15. If no inspections are conducted, the error of the EDS model grows in time and for decreasing FDF. At the last year, the relative error is 3.5% for $FDF = 5$ and 2% for $FDF = 10$, which is below the 5% maximum model error recommended by JCSS [30]. Departing from the undamaged system increases the likelihood of combinations of failure modes that the EDS model can only approximate. Thus, in general lines, the error increases for increasing deterioration; in other words, for decreasing β_{DS}. When inspections are conducted, the deviation between the two models tends to be lower for decreasing inspection interval Δt_I. It is nonetheless noted that a significant part of the deviation is attributed to the variability associated with the sampling technique. This part of the deviation would disappear if the same inspection outcome histories would be sampled for both models.

We argue in this article that the target safety level for the deteriorated structure should be somewhat close to the one prescribed for the non-deteriorated one. If that criterion is employed, the use of the EDS model incurs only a small error in comparison to assessing the complete structural system.

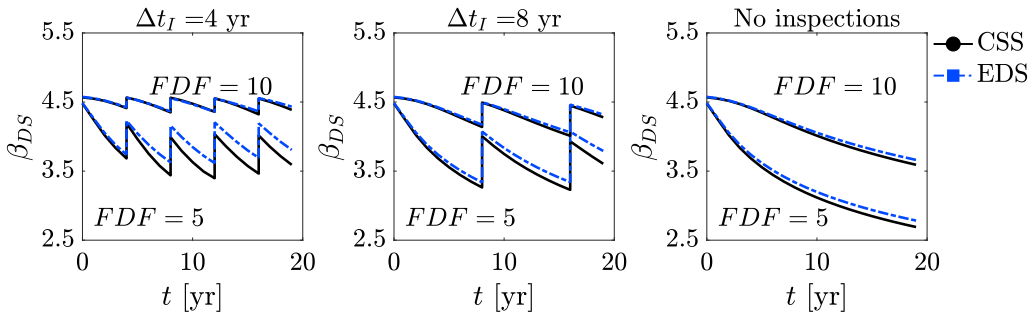

Fig. A.15. Annual reliability index of the system β_{DS}, estimated from the complete structural system (CSS) model and the equivalent Daniels system (EDS) model.

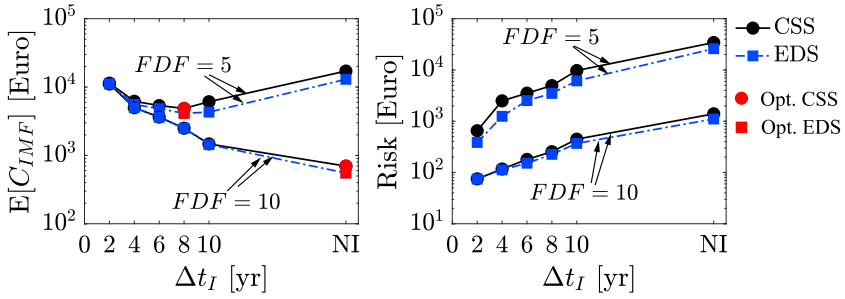

Fig. A.16. Results of the computation of the expected cost of inspections, maintenance and failure risk $\mathbb{E}[C_{IMF}]$ and the failure risk obtained by assessing the complete structural system and the equivalent Daniels system (EDS) are compared.

A.2. Accuracy of the estimation of risk-based inspection planning

The performance of the EDS model is also tested for optimal risk-based inspection planning. The individual costs in Table 2 are used to build the cost model. The expected total inspection and maintenance cost $\mathbb{E}[C_{IMF}]$ and the risk of failure are plotted in Fig. A.16 for different inspection intervals Δt_I. It is seen that both models predict the same optimal inspection interval, which is eight years for $FDF = 5$ and not to conduct inspections for $FDF = 10$. It is noted that due to the error in the estimation of the reliability index (and consequently the risk of failure) the EDS will assess different optimal inspection interval for some situations. This disagreement is expected to be more accentuated when the $\mathbb{E}[C_{IMF}]$ curve is flatter around the optimal decision due to the optimisation problem being ill-conditioned.

A.3. Conclusion of the validation example

It is concluded that the use of the EDS representation results in an estimation of the reliability index that is sufficiently accurate for the reliability- and risk-based prescription of optimal mitigation of fatigue failure risk for standardisation purposes.

References

[1] NORSOK. Design of steel structures. Standard N-004, Lysaker, Norway: Standards Norway; 2004.

[2] CEN. Eurocode 3: Design of steel structures Part 1-9: Fatigue. Standard EN 1993-1-9:2005: E, Brussels, Belgium: European Committee for Standardization; 2005.

[3] ISO. Petroleum and natural gas industries — Fixed steel offshore structures. Standard ISO 19902:2020, Geneva, Switzerland: International Organization for Standardization; 2020.

[4] DNV-GL. Fatigue design of offshore steel structures. Recommended practice DNVGL-RP-C203, 2016.

[5] Hobbacher AF. Recommendations for fatigue design of welded joints and components. IIW-2259-15, Springer International Publishing, International Institute of Welding; 2016.

[6] Schafhirt S, Zwick D, Muskulus M. Two-stage local optimization of lattice type support structures for offshore wind turbines. Ocean Eng 2016;117:163–73. http://dx.doi.org/10.1016/j.oceaneng.2016.03.035.

[7] Moan T. Reliability-based management of inspection, maintenance and repair of offshore structures. Struct Infrastruct Eng 2005;1(1):33–62. http://dx.doi.org/10.1080/15732470412331289314.

[8] Mendoza J, Bismut E, Straub D, Köhler J. Risk-based fatigue design considering inspections and maintenance. ASCE ASME J Risk Uncertain Eng Syst A Civ Eng 2020;7(1):04020055. http://dx.doi.org/10.1061/AJRUA6.0001104.

[9] Madsen HO, Sørensen JD. Probability-based optimization of fatigue design, inspection and maintenance. In: Int. symp. on offshore structures. 1990.

[10] Cramer EH, Friis-Hansen P. Reliability-based optimization of multi-component welded structures. J Offshore Mech Arct Eng 1994;116(4):233–8. http://dx.doi.org/10.1115/1.2920157.

[11] Sørensen JD. Reliability-based calibration of fatigue safety factors for offshore wind turbines. Int J Offshore Polar Eng 2011;22(3):234—241.

[12] Gintautas T, Sørensen JD. Reliability-based inspection planning of 20 MW offshore wind turbine jacket. Int Jof Offshore Polar Eng 2018;28(03):272–9. http://dx.doi.org/10.17736/ijope.2018.il53.

[13] Márquez-Domínguez S, Sørensen JD. Fatigue reliability and calibration of fatigue design factors for offshore wind turbines. Energies 2012;5(6):1816–34. http://dx.doi.org/10.3390/en5061816.

[14] Yang Y, Peng J, Cai C, Zhou Y, Wang L, Zhang J. Time-dependent reliability assessment of aging structures considering stochastic resistance degradation process. Reliab Eng Syst Saf 2022;217:108105. http://dx.doi.org/10.1016/j.ress.2021.108105.

[15] Luque J, Hamann R, Straub D. Spatial probabilistic modeling of corrosion in ship structures. ASCE-ASME J Risk Uncertain Eng Syst Part B: Mech Eng 2017;3(3):031001. http://dx.doi.org/10.1115/1.4035399.

[16] Mendoza J, Paglia J, Eidsvik J, Köhler J. Value of information of in situ inspections of mooring lines. Proc Instit Mech Eng Part O: J Risk Reliab 2021;235(4):556–67. http://dx.doi.org/10.1177/1748006X20987404.

[17] Adumene S, Khan F, Adedigba S, Zendehboudi S. Offshore system safety and reliability considering microbial influenced multiple failure modes and their interdependencies. Reliab Eng Syst Saf 2021;215:107862. http://dx.doi.org/10.1016/j.ress.2021.107862.

[18] Yuan X-X, Higo E, Pandey MD. Estimation of the value of an inspection and maintenance program: A Bayesian gamma process model. Reliab Eng Syst Saf 2021;216:107912. http://dx.doi.org/10.1016/j.ress.2021.107912, URL https://www.sciencedirect.com/science/article/pii/S0951832021004270.

[19] Iannacone L, Sharma N, Tabandeh A, Gardoni P. Modeling time-varying reliability and resilience of deteriorating infrastructure. Reliab Eng Syst Saf 2022;217. http://dx.doi.org/10.1016/j.ress.2021.108074.

[20] Straub D, Der Kiureghian A. Reliability acceptance criteria for deteriorating elements of structural systems. J Struct Eng 2011;137(12):1573–82. http://dx.doi.org/10.1061/(ASCE)ST.1943-541X.0000425.

[21] Hohenbichler M, Rackwitz R. First-order concepts in system reliability. Struct Saf 1982;1(3):177–88. http://dx.doi.org/10.1016/0167-4730(82)90024-8.

[22] Gharaibeh ES, Frangopol DM, Onoufriou T. Reliability-based importance assessment of structural members with applications to complex structures. Comput Struct 2002;80(12):1113–31. http://dx.doi.org/10.1016/S0045-7949(02)00070-6.
[23] Daniels HE. The statistical theory of the strength of bundles of threads. I. Proc R Soc Lond Series A. Math Phys Sci 1945;183(995):405–35.
[24] Gollwitzer S, Rackwitz R. On the reliability of Daniels systems. Struct Saf 1990;7(2):229–43. http://dx.doi.org/10.1016/0167-4730(90)90072-W.
[25] Straub D, Schneider R, Bismut E, Kim H-J. Reliability analysis of deteriorating structural systems. Struct Saf 2020;82:101877. http://dx.doi.org/10.1016/j.strusafe.2019.101877.
[26] Thoft-Christensen P, Sørensen J. Optimal strategy for inspection and repair of structural systems. Civ Eng Syst 1987;4(2):94–100.
[27] Memarzadeh M, Pozzi M, Zico Kolter J. Optimal planning and learning in uncertain environments for the management of wind farms. J Comput Civ Eng 2014;29(5):04014076. http://dx.doi.org/10.1061/(ASCE)CP.1943-5487.0000390.
[28] Luque J, Straub D. Risk-based optimal inspection strategies for structural systems using dynamic Bayesian networks. Struct Saf 2019;76:68–80. http://dx.doi.org/10.1016/j.strusafe.2018.08.002.
[29] ISO. General principles on reliability for structures. Standard ISO 2394:2015, Geneva, Switzerland: pub-ISO, International Organization for Standardization; 2015.
[30] JCSS. Probabilistic model code. Part 1 – basis for structural design. Joint Committee on Structural Safety; 2001.
[31] CEN. Eurocode 0: Basis of structural design. Standard EN 1990:2002, Brussels, Belgium: CEN, European Committee for Standardization; 2002.
[32] Efthymiou M, van de Graaf JW. Reliability and (re)assessment of fixed steel structures. In: International conference on offshore mechanics and arctic engineering, Vol. 44359. 2011, p. 745–54.
[33] HSE. Comparison of fatigue provisions in codes and standards. Offshore technology report 2001/083, Health and Safety Executive; 2001.
[34] Aggarwal R, DoIan D, Cornell C, et al. Development of bias in analytical predictions based on behavior of platforms during hurricanes. In: Offshore technology conference. OTC, (8077):Houston, Texas, USA; 1996, p. 433–44.
[35] Stahl B, Aune S, Gebara JM, Cornell CA. Acceptance criteria for offshore platforms. J Offshore Mech Arct Eng 2000;122(3):153–6. http://dx.doi.org/10.1115/1.1287344.
[36] Bismut E, Straub D. Optimal adaptive inspection and maintenance planning for deteriorating structural systems. Reliab Eng Syst Saf 2021;215:107891. http://dx.doi.org/10.1016/j.ress.2021.107891.
[37] Luque J, Straub D. Reliability analysis and updating of deteriorating systems with dynamic Bayesian networks. Struct Saf 2016;62:34–46. http://dx.doi.org/10.1016/j.strusafe.2016.03.004.
[38] Bismut E, Luque J, Straub D. Optimal prioritization of inspections in structural systems considering component interactions and interdependence. In: Proc. 12th international conference on structural safety & reliability ICOSSAR 2017, Vienna, Austria. 2017.
[39] Själander M, Jahre M, Tufte G, Reissmann N. EPIC: An energy-efficient, high-performance GPGPU computing research infrastructure. 2019, arXiv:1912.05848.